A Spectroscopic Study of Solvent Reorganization Energy: Dependence on Temperature, Charge Transfer Distance, and the Type of Solute−Solvent Interactions

Peter Vath and Matthew B. Zimmt*

Department of Chemistry, Brown University, Providence, Rhode Island 02912

Received: October 14, 1999; In Final Form: December 30, 1999

The dependence of the free energy gap, $\Delta G(S_0 \rightarrow CT)$, and of the solvent reorganization energy, λ_S, on solvent, donor/acceptor separation, and temperature are determined from analyses of the intramolecular charge transfer absorption and emission bands from **1** and **2**. The following trends are observed: (a) for either probe molecule, differences in the CT state energies among the various solvents are attended by nearly identical magnitude (but opposite sign) differences in the solvent reorganization energies. This correlation is observed for solvents in which the most significant electrostatic moment is a dipole or a quadrupole. (b) Solvents with nearly zero dipole moments but large quadrupole moments (8−11 D-Å) solvate the CT state as effectively as moderately dipolar solvents ($\mu \approx 1-2$ D). (c) Larger charge separation distances produce larger solvent reorganization energies in the nonalkane solvents. The ratios of the solvent reorganization energies λ_S**(2)**/λ_S**(1)** are roughly the same in the dipolar and quadrupolar solvents. (d) Changes in both ΔG and λ_S upon increasing the temperature are consistent with a decrease in the solvent polarity. The absolute values of the temperature derivatives lie between 0.5 and 2.0 meV/K. In contrast to the correlated variation of $\Delta G(S_0 \rightarrow CT)$ and λ_S from solvent to solvent (i.e., $\Delta G_{\text{solvent A}} - \Delta G_{\text{solvent B}} \approx -(\lambda_{S,\text{solvent A}} - \lambda_{S,\text{solvent B}})$, the ratio $(\partial\lambda_S/\partial T)/(\partial\Delta G/\partial T) \sim -(0.7-0.9)$. A simple continuum model, using dielectric constant data, is unable to reproduce the solvent and temperature dependence of $\Delta G(S_0 \rightarrow CT)$ and λ_S. A more detailed molecular model produces reasonable estimates of these two quantities across a wide range of solvents at 300 K but overestimates their temperature variation.

I. Introduction

The kinetic barrier in condensed phase electron transfer (ET) reactions is strongly influenced by the solvent reorganization energy, λ_S.[1] Fluctuations in the positions and orientations of solvent molecules toward "product-like" configurations induce crossings of the reactant and product surfaces. These productive motions of the initial state along the solvent coordinate are attended by an energy increase that comprises the activation barrier. The curvature along the solvent coordinate, which is fundamentally related to λ_S,[2] is determined by the intrinsic solvent−solvent interaction potentials.[3] These change with solvent, temperature, and pressure. Thus, any investigation of ET kinetics involving variation of these parameters requires a detailed understanding of their influence on the solvent reorganization energy.

Direct, experimental determination of the solvent reorganization energy is not a simple task. The most credible information comes from analyses of (i) optical charge transfer bands found in transition-metal-based[4] and organic[5] intervalence molecules and (ii) charge transfer absorption and emission band shapes found in some excited-state electron transfer systems.[6] As the majority of nonadiabatic electron transfer systems do not exhibit detectable charge transfer transitions, λ_S is not known a priori. Instead, reference is regularly made to one of the numerous theoretical approaches[7] when a numerical value of λ_S is required. The simplest continuum expressions for λ_S, originally advanced by Marcus and Hush, are widely used with apparent success. However, we recently demonstrated that simple continuum models predict the wrong sign of $\partial\lambda_S/\partial T$ in the polar solvent acetonitrile.[8] Furthermore, in our efforts to extract donor−acceptor electronic coupling matrix elements |V| from the temperature dependence of nonadiabatic electron-transfer rate constants, we found that different models for λ_S produced significantly different values of |V|.[9] The model dependence arose from divergent predictions of the *temperature dependence* of λ_S, including both negative and positive values of $\partial\lambda_S/\partial T$.

Clearly, it is important to measure λ_S and $\partial\lambda_S/\partial T$ and to ascertain which solvent properties contribute significantly to solvation. These must be properly incorporated in models to generate accurate predictions of the solvation energy, the solvent reorganization energy, and their temperature dependences. This manuscript is a step in this direction. Experimental values of λ_S are reported as a function of solvent, temperature, and donor−acceptor separation. The results provide a benchmark for the continuing evolution and evaluation of λ_S models. Currently, no single model works best for all ET geometries and solvents, but clear failures of various models are demonstrated.

Numerous solute−solvent interactions are altered by solvent motions and, therefore, contribute to λ_S. In aprotic solvents with large dipole moments, the primary contribution to λ_S arises from the solute−solvent dipole−dipole interaction's modulation by solvent reorientation.[2c,10] In weakly and non-dipolar solvents, solute interactions with higher order solvent multipole moments (quadrupole, octapole, etc.) are modulated by solvent reorientation and make significant contributions to λ_S.[11] In addition to rotation, translation of solvent molecules near the solute alter solute−solvent electrostatic interactions. ET-induced changes in the solute's electric field gradient perturb the local solvent

* Corresponding author.

10.1021/jp993667k CCC: $19.00
Published on Web 03/02/2000

density.[12] This change in the solute−solvent radial distribution function (alternately referred to as solvent density fluctuations, electrostriction, or solvent translation) contributes to λ_S via modulation of solute−solvent and solvent−solvent dipolar and multipolar interactions.[3c,7e,13] Interestingly, interactions between the solute and solvent molecule polarizability are also modulated by density changes, thus producing polarizability contributions to λ_S.[8,14]

Simple continuum models employ the dielectric constant and refractive index to evaluate λ_S.[15]

$$\lambda_S(\text{Marcus}) = \frac{e^2}{2}\left(\frac{1}{r_A} + \frac{1}{r_D} - \frac{2}{R_{CC}}\right)\left(\frac{1}{n^2} - \frac{1}{\epsilon_S}\right) \quad (1)$$

$$\lambda_S(\text{dipole}) = \frac{\mu^2}{a^3}\left(\frac{\epsilon_S - 1}{2\epsilon_S + 1} - \frac{n^2 - 1}{2n^2 + 1}\right) \quad (2)$$

While these bulk properties may be influenced somewhat by solvent translations and higher order electrostatic moments, the contributions to λ_S from these highly localized solvent features are not adequately reproduced by eqs 1 and 2. A demonstration of this flaw in the continuum models can be found in nondipolar solvents, e.g., aromatics and dioxane, for which experimental solvent reorganization energies are significantly larger than λ_S predicted by eqs 1 and 2.[11a] Recently, modifications to these equations have been proposed in an attempt to introduce effective nondipolar solvation terms within continuum models.[7c]

Alternative models for λ_S have been developed which incorporate molecular descriptions of the solvent. Molecular dynamics calculations of λ_S have been effected using realistic solute−solvent and solvent−solvent potentials.[16] Analytic theories for λ_S, based on dipolar, polarizable hard sphere solvents, have been developed[3c,7d,10b,11d,13,14] and shown to reproduce important characteristics of λ_S, including its temperature dependence.[8] Some of the molecular theories are being modified to incorporate contributions from solvent quadrupoles.[11b−d] Most theoretical models have been developed for limiting electron transfer topologies, i.e., electron transfer resulting in formation of a point dipole or widely separated ions. As the charge distributions in real systems often fall between these limits, the impact of the charge transfer distance on λ_S and $\partial\lambda_S/\partial T$ warrants experimental investigation.

In an attempt to address some of the issues raised above, we have investigated the temperature dependence of the charge transfer (CT) absorption and emission bands of molecules[17] **1** and **2** in a variety of solvents. The distance from the S atom to the ring substituted

1

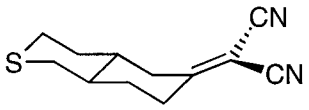

2

alkene C is 3.15 Å in **1** and 5.49 Å in **2**. We previously demonstrated that a molecular theory employing dipolar, polarizable hard sphere solvents does a good job of predicting the temperature dependence of λ_S and $\Delta G°$ for **1** in acetonitrile.[8] The good agreement between experiment and theory in this system arises, in part, because the difference between the ground and excited-state charge distribution of **1** is reasonably simulated as a point dipole and because acetonitrile has a very small quadrupole moment. Characterization of λ_S and $\partial\lambda_S/\partial T$ for **2** in acetonitrile will help to characterize the transition from dipolar to ion pair models in a solvent with predominantly dipolar solvation. Studies in the nondipolar solvents benzene and dioxane were effected with the aim of characterizing the temperature and distance[11b,c] dependence of λ_S in solvents where solvation by quadrupole moments should predominate. The studies in the mildly polar solvents diethyl ether and tetrahydrofuran were included to characterize the behavior of systems with comparable dipolar and quadrupolar contributions to λ_S.

II. Experimental Section

Molecules **1** and **2** were prepared according to literature methods[17] with one exception. We were unable to effect the reduction of the α,β double bond of ketone **3**

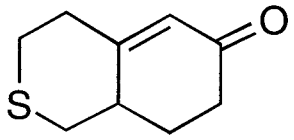

3

with H_2 over a variety of Pd-supported catalysts. Reduction was effected using $Na_2S_2O_4$ in water containing Aliquat and $NaHCO_3$, producing predominantly the *trans*-6-thiadecalone.[18] The ^{13}C and ^1H NMR data were in good agreement with published spectral data.[17] The trans ketone was isolated by chromatography and converted[17] to **2**.

Excitation and emission spectral line shapes, measured as photons/s^{-1} nm^{-1}, were determined as a function of temperature using a SPEX F111 Fluorolog fluorometer. Emission spectra were corrected for the response of the emission monochromator and detector. Excitation spectra were corrected for the wavelength dependence of the lamp spectral output and transmission of the monochromator (excitation correction profile) using the SPEX quantum counter. The excitation spectrum of **2** extended below 250 nm, where the lamp output is extremely weak. The quantum-counter-derived excitation profile at $\lambda < 250$ nm was heavily contaminated by stray visible light reflected off the monochromator grating. A Hoya U330 filter (band-pass 230−420 nm) was inserted prior to the exit slit of the monochromator. This reduced, but did not eliminate, the visible light reaching the quantum counter and sample chamber. As this light did not excite the CT band of **2**, the excitation correction profile was corrected for the leakage light by fitting the wavelength dependence of the data on both sides of the filter band-pass (the data in these regions should be zero) and subtracting the resulting, best-fit function from the measured excitation correction profile. The resulting excitation profile was divided into the measured excitation spectrum to generate the corrected excitation spectrum. In cases where signal intensity from the solvent was greater than 5% of the excitation or emission signal from the solute, the solvent-only data was subtracted from the solute data prior to processing with the emission or excitation correction factors.

Transformation of emission and excitation spectral profiles from nm to cm^{-1} units was achieved through multiplication of the intensity at each wavelength by λ^2. Absorption spectra were directly converted to cm^{-1} units. The emission Franck−Condon (FC) line shapes were extracted from the spectra (vs cm^{-1}) through division by $\bar{\nu}$. The excitation (absorption) Franck−Condon (FC) line shapes were extracted from the spectra (vs

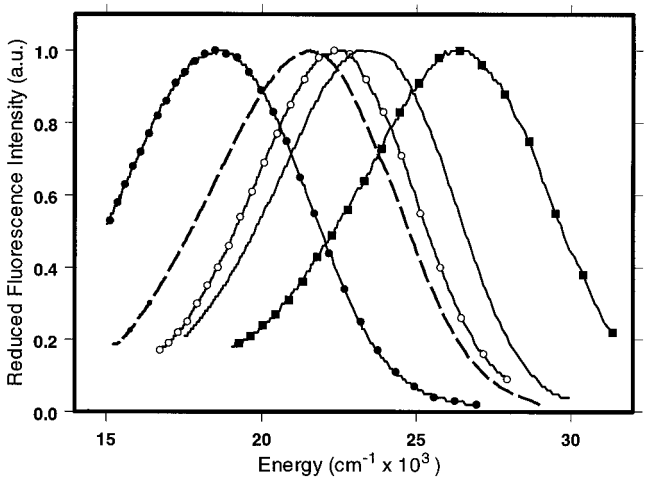

Figure 1. Room-temperature reduced emission spectra from **1** in MeCN (—•—), dioxane (- - -), benzene (—○—), ether (—), and 2-methylbutane (—■—).

cm^{-1}) through multiplication by $\bar{\nu}$. Both extraction procedures presume that the transition moment is proportional to $\bar{\nu}^{-1}$, thus converting the $\bar{\nu}^3$ and $\bar{\nu}$ factors, appearing in the Einstein expressions, to $\bar{\nu}$ and $\bar{\nu}^{-1}$, respectively (see Discussion section).[19] The maximum of each reduced spectrum was determined by fitting the top 20% of the line shape to a cubic expression.

Solvents were dried over Na or P_2O_5 and distilled through an 8-in. vigreux or fractionation column. Samples were prepared in 1 cm path length fused Suprasil cells fitted with high vacuum seals. Sample optical densities were less than 0.4 for emission spectra and 0.1 for excitation spectra, thus ensuring linearity and additivity. The sample temperature was controlled using an aluminum cell holder, cooled or heated by 2-propanol or water circulated from a constant-temperature bath. The sample temperature was determined using a Cole Parmer Digital Thermometer and a Type T disk probe that was in direct contact with the fluorescence cuvette.

III. Results

A. Excitation and Emission Maximums. Verhoeven and co-workers[17] previously described the dependence of **1** and **2**'s CT emission maximum on the solvent polarity, as gauged by the solvent dielectric properties. Figure 1 illustrates that the Franck—Condon emission maximum for **1** at 300 K in the "nonpolar" solvent dioxane ($\epsilon_S = 2.2$) lies 2/3 of the way between the FC emission maximum in the nonpolar alkane solvent 2-methylbutane ($\epsilon_S = 1.8$) and the highly polar solvent acetonitrile ($\epsilon_S = 37$). Similarly, the FC emission maximum for **1** in benzene ($\epsilon_S = 2.3$) lies roughly halfway between the 2-methylbutane and acetonitrile maximums: further red shifted than the FC emission maximum in the weakly polar solvent diethyl ether ($\epsilon_S = 4.3$). Judging by their red shifted emission maximum, benzene and dioxane are more "polar" solvents than ether. Table 1 lists the FC emission maximum for **1** and **2** at 300 K in the six solvents. To determine spectroscopic values of λ_S and ΔG with reasonable confidence,[20] both the CT emission and CT absorption bands must be determined. The CT absorption band from **1** is reasonably separated from the $S_0 \rightarrow S_1$ transition of acceptor group and from most of the solvents' absorption bands. However, for **1** in benzene and for **2** in all the solvents, the CT absorption band is overlapped by acceptor and/or by solvent transitions. Fortunately, Verhoeven[17] previously demonstrated that excitation into the acceptor absorption band produces no emission and, as a consequence, the CT absorption band can be detected, without interference, by measuring the fluorescence excitation spectrum. Table 1 lists the FC excitation maximum determined in this manner for **1** and **2** at 300 K. In contrast to the emission spectra, the excitation spectra exhibit minimal solvent dependence: $\langle\bar{\nu}_{EXC}(1)\rangle = 34.30 \pm 0.27$ kK, $\langle\bar{\nu}_{EXC}(2)\rangle = 37.77 \pm 0.31$ kK.

The CT excitation and emission spectra of **1** and **2** were also determined as a function of temperature in the six solvents (Figure 2). The CT emission bands exhibit much larger thermochromism than the corresponding CT excitation bands. The temperature dependence of both FC maximums are reasonably fit to straight lines (Figure 3). The slopes of the best-fit linear regressions are listed in Table 2. For **1** (and **2**), the temperature dependence of the FC emission maximum is nominal in 2-methylbutane and increases in the order benzene, dioxane, ethyl ether, tetrahydrofuran. Acetonitrile breaks the trend of increasing slope with increasing dielectric constant: exhibiting a temperature dependence of the FC emission maximum that is less than half of that in THF. The FC excitation maximum slopes exhibit no significant trends with solvent.

B. Reaction Free Energy, Solvent and Vibrational Reorganization Energies. To a first approximation[19] (vide infra), the energies of the FC excitation and emission maximums may be related to the solvent reorganization energy, λ_S, the vibrational reorganization energy, λ_V, and the free energy difference between the ground and CT state, ΔG, as

$$hc\bar{\nu}_{EXC} = \lambda_S + \lambda_V + \Delta G \quad hc\bar{\nu}_{EM} = \Delta G - \lambda_S - \lambda_V \quad (3)$$

Determination of λ_S and ΔG from the FC maximum data requires an estimate of λ_V. AM1 calculations were used to estimate λ_V as one-half of the sum of the energies required to distort the ground state of **1** to the equilibrium geometry of $\mathbf{1}^{+\bullet}$ and to the equilibrium geometry of $\mathbf{1}^{-\bullet}$ and the energies required to distort the equilibrium geometries of $\mathbf{1}^{+\bullet}$ and of $\mathbf{1}^{-\bullet}$ to the equilibrium geometry of the ground state. Calculated in this manner, λ_V was determined to be 0.45 eV (3630 cm^{-1}) for **1** and to be 0.54 eV (4360 cm^{-1}) for **2**. Using these estimates of λ_V and eqs 3, values of ΔG and λ_S for **1** and **2** in the six solvents were determined (Table 3).

The results in Table 3 warrant two comments at this point. (a) The solvents have been arranged in order of increasing stabilization of the CT state, relative to the ground state. This represents a thermodynamic or "total polarity" ordering as opposed to conventional polarity ordering based on dielectric constant. This thermodynamic polarity order is slightly different than one based on $E_T(30)$ values (diethyl ether is slightly more polar than benzene according to $E_T(30)$ values) and is quite different than one based on π^* values (benzene, dioxane, and THF are very similar based on π^*).[21] (b) The calculated vibrational reorganization energies comprise 85% of the Stokes shift for **1** and 95% of the Stokes shift for **2** in 2-methylbutane. The corresponding values of the solvent reorganization energy are quite small, consistent with other experimental results[11a,22] in alkane solvents. There is no obvious reason why λ_S in 2-methylbutane should be bigger for **1** (the smaller CT distance) than for **2**. This "conundrum" likely provides a measure of the errors arising from the calculation of λ_V using the AM1 method.[23] While such error affects the magnitude of the determined λ_S, it exerts no impact on the solvent polarity or λ_S ordering.

The temperature dependence of ΔG and λ_S may be determined from the data in Table 2 and eqs 3. The values of $\partial\Delta G/\partial T$ and $\partial\lambda_S/\partial T$ (Table 4) are unaffected by errors in the calculated λ_V, provided the latter quantity is temperature independent.

TABLE 1: Franck−Condon Excitation and Emission Maximums for 1 and 2 at 300 K

solvent	$\bar{\nu}_{EXC}(1)$ (kK)	$\bar{\nu}_{EM}(1)$ (kK)	$\bar{\nu}_{EXC}(2)$ (kK)	$\bar{\nu}_{EM}(2)$ (kK)
2-methylbutane[a]	34.75 ± 0.24	26.35 ± 0.14	38.20 ± 0.29	28.98 ± 0.17
diethyl ether	34.30 ± 0.23	23.42 ± 0.11	37.58 ± 0.28	23.23 ± 0.11
benzene	34.05 ± 0.23	22.39 ± 0.10	[b]	[b]
dioxane	34.15 ± 0.23	21.55 ± 0.09	37.74 ± 0.28	21.33 ± 0.09
tetrahydrofuran	34.23 ± 0.23	19.73 ± 0.08	37.40 ± 0.28	18.49 ± 0.07
acetonitrile	34.27 ± 0.23	18.57 ± 0.07	37.91 ± 0.28	16.05 ± 0.05

[a] Measured at 295 K in 2-methylbutane. [b] Solvent overlap with absorption band too severe to allow investigation.

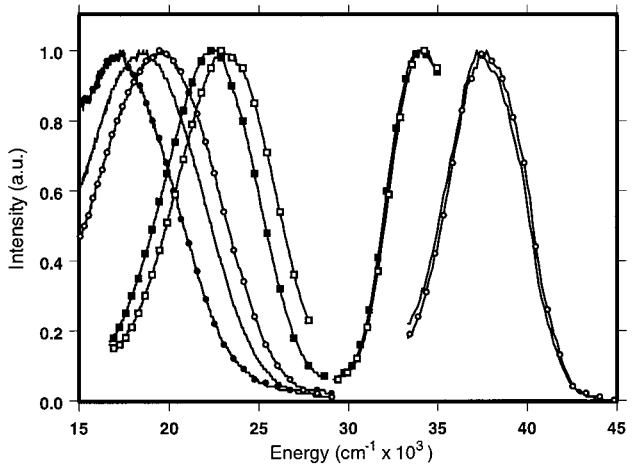

Figure 2. Reduced excitation and emission spectra as a function of temperature: **1** in benzene at 348 K (−□−), 300 K (−■−); **2** in THF at 348 K (−○−), 300 K (—), 248 K (−●−) (emission only).

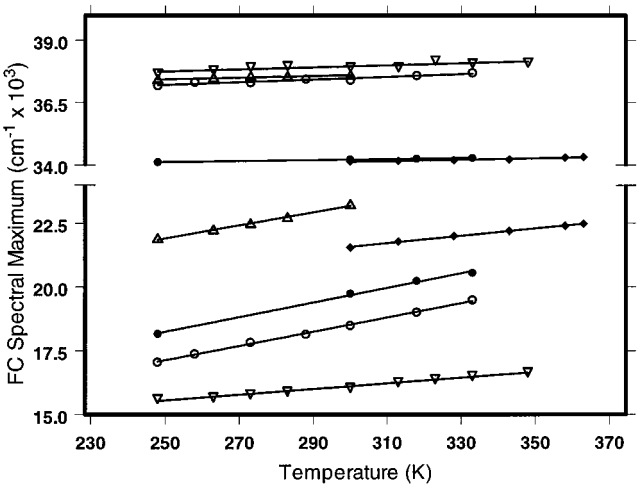

Figure 3. Temperature-dependent reduced excitation and emission maximum data and the best-fit linear regression lines. The excitation spectral data are displayed above the *y*-axis break; the emission spectral data are displayed below the *y*-axis break. The closed symbols are data from **1** and the open symbols are data from **2**. Acetonitrile (▽), dioxane (◆), ethyl ether (△), THF (○,●).

Excluding the data in 2-methylbutane, the average value of the ratio $(\partial\lambda_S/\partial T)/(\partial\Delta G/\partial T)$ is −0.73 ± 0.07 for **1** and −0.70 ± 0.16 for **2**.

C. CT Emission Band Shape Analysis. The Franck−Condon excitation and emission line shapes may be simulated in order to obtain estimates of the solvent reorganization energy. Within the single quantized mode semiclassical model, the line shape and position of these profiles are determined by ΔG, λ_S, λ_V, and the effective quantized mode spacing, $\hbar\omega$.[19] Simulation of emission profiles without constraints on any of the four parameters leads to multiple, and widely differing solutions of similar "fit" quality. Instead, the Franck−Condon emission profiles from **1** and **2** were simulated at each temperature using $\Delta G(T)$ determined from the Stokes shift analyses. Although Mertz[24] has criticized the use of Stokes shifts (eqs 3) to determine λ_S (vide infra), his analyses indicate that the method generates reasonable values of ΔG. Simulations were performed using $\lambda_V = 0.45$ eV for **1** and $\lambda_V = 0.54$ eV for **2**. Best-fit values of $\hbar\omega$ and $\lambda_S(T)$ were obtained at each temperature. Values of $\hbar\omega$ between 0.2 and 0.25 eV provided reasonable fits to the data. The average value of $\hbar\omega$, 0.225 eV for **1** and 0.21 eV for **2**, was used to determine λ_S(300 K) and $\partial\lambda_S/\partial T$ in each solvent (Table 5, See the Supporting Information for the equation employed and examples of fits). The λ_S(300 K) values derived from line shape analyses are larger than the values obtained from the Stokes shift (average increase: 0.08 eV). The calculated temperature dependence of λ_S is larger, such that the average value of $(\partial\lambda_S/\partial T)/(\partial\Delta G/\partial T)$ is −0.9.

IV. Discussion

Polarizability and dipole, quadrupole, and higher order electrostatic moments are the primary solvent molecule properties responsible for effecting solvation. The results in Tables 3 and 4 provide some insights as to their efficacy of interaction with CT states: (a) Some nondipolar solutes (benzene, dioxane) are effective at stabilizing CT states, while others (2-methylbutane) are not. This may be understood by reference to a number of recent investigations that demonstrate and explore solvation arising from solvent quadrupole[11] moments. The effective axial quadrupole moments[11a] $\langle Q\rangle$ are 0.7 D-Å in 2-methylbutane, 2.5 D-Å in acetonitrile, 5.4 D-Å in THF, 8.4 D-Å in benzene, and 11.7 D-Å in dioxane. The interaction energy between a solute dipole and a solvent quadrupole scales,[11d] roughly, as $\langle Q\rangle^2$. Thus, quadrupolar solvation by benzene and dioxane should be considerably larger than by 2-methylbutane, THF, or acetonitrile.[25] Dipolar solvation should be larger for the latter two solvents. The ΔG values in Table 3 confirm that dipolar solvation in solvents with large dipole moments is more effective than quadrupolar solvation. Remarkably, dioxane provides about 75% of the excess solvation (defined as ΔG(2-methylbutane) − ΔG(solvent)) provided by THF. Simple dielectric continuum models fail to predict the considerable stabilization of the CT state (in **1** and **2**) provided by the large quadrupole, nondipolar solvents. For that matter, continuum models do only a fair job of predicting the relative solvation magnitudes effected by the dipolar solvents.[26] (b) The magnitude of λ_S in the quadrupolar solvents, benzene and dioxane, is greater than in diethyl ether. This result is in accord with recent time-resolved Stokes shift determinations of λ_S for coumarin dyes,[11a] but contradicts the predictions of continuum models. (c) Without regard for the types of solvent−solute interactions that are active, solvents that effect increased solvation of the solute CT state suffer nearly identical increases in the (neutral ↔ CT) solvent reorganization energy. Plots of λ_S vs ΔG are linear, with slopes of 1.03 for both **1** and **2** (Figure 4).[27] Continuum models[28] predict that variations of ΔG (neutral → CT) with solvent dielectric constant are attended by identical changes in λ_S provided the solvent

TABLE 2: Franck−Condon Excitation and Emission Maximum Temperature Dependence

solvent	$\partial\bar{\nu}_{EXC}(1)/\partial T$ (cm^{-1}/K)	$\partial\bar{\nu}_{EM}(1)/\partial T$ (cm^{-1}/K)	$\partial\bar{\nu}_{EXC}(2)/\partial T$ (cm^{-1}/K)	$\partial\bar{\nu}_{EM}(2)/\partial T$ (cm^{-1}/K)
2-methylbutane	3.2 ± 0.2	-0.3 ± 0.5	8.2 ± 1.4	4.0 ± 1.4
diethyl ether	3.8 ± 0.7	18.6 ± 0.5	3.4 ± 0.6	25.8 ± 0.9
benzene	2.2 ± 0.4	14.4 ± 0.7	[a]	[a]
dioxane	2.9 ± 0.4	14.4 ± 0.4	0.9 ± 0.7	20.9 ± 0.7
tetrahydrofuran	2.1 ± 0.1	28.6 ± 0.1	5.5 ± 0.7	27.9 ± 0.6
acetonitrile	1.9 ± 0.1	14.7 ± 0.3	4.2 ± 0.9	11.2 ± 0.5

[a] Not determined.

TABLE 3: ΔG ($S_0 \rightarrow$ CT) and λ_S for 1 and 2 at 300 K[a]

solvent	ΔG (1) (eV)	$\lambda_S(1)$ (eV)	ΔG (2) (eV)	λ_S (2) (eV)
2-methylbutane[b]	3.79	0.07	4.16	0.03
diethyl ether	3.58	0.22	3.77	0.35
benzene	3.50	0.27	[c]	[c]
dioxane	3.45	0.33	3.66	0.48
tetrahydrofuran	3.34	0.45	3.46	0.63
acetonitrile	3.28	0.52	3.34	0.82

[a] Uncertainties in ΔG and λ_S are ± 0.02 eV except for **2** in 2-methylbutane for which the uncertainties are ± 0.03 eV. [b] Measured at 295 K. [c] Solvent overlap too severe to allow investigation.

refractive index remains constant. Based on the present results, the correlation is more general, extending to solvents for which ϵ_S does not provide a good measure of CT state solvation, and is only weakly affected by the solvent refractive index.[29] (d) The energetic cost of extending the charge separation distance (i.e., $\Delta G(2) - \Delta G(1)$) decreases with the ability of the solvent to stabilize the CT state (i.e., with "total polarity"). In the most polar solvent investigated, acetonitrile, the decreased D^+/A^- Coulomb interaction at the larger separation is nearly compensated by increased CT state solvation. (e) The solvent reorganization energy increases with increasing CT distance: by a factor of 1.43 ± 0.15 (Tables 3 and 5) from **1** to **2**. There is no statistically significant difference between the distance dependence of λ_S found in the quadrupolar solvent dioxane and the dipolar solvents ethyl ether, tetrahydrofuran, or acetonitrile. Perng[11b,c] predicted that λ_S in quadrupolar solvents should be distance independent at large D/A separations (>7 Å in their calculations) and decrease at shorter D/A distances. The distance-independent λ_S regime clearly was not attained with the two, rather short, D/A separations investigated here. (f) Higher temperatures reduce the efficacy of CT state solvation: $\Delta G(S_0 \rightarrow CT)$ increases and λ_S decreases. The apparent entropy change attending formation of the charge transfer state, $-\partial\Delta G/\partial T$, is nominal in 2-methylbutane but large and negative in the other solvents: e.g., -44 and -46 cal/mol − K in tetrahydrofuran for **1** and **2**, respectively. The entropy difference, $-T(\Delta S(\mathbf{2}) - \Delta S(\mathbf{1}))$, constitutes nearly the entire free energy difference $\Delta G(2) - \Delta G(1)$ (at 300 K) in ethyl ether. With increasing solvent polarity, the entropy difference is responsible for less of the observed free energy difference (on an absolute or percentage basis).[30] (g) As noted above, the ratio $(\partial\lambda_S/\partial T)/(\partial\Delta G/\partial T)$ lies between -0.7 and -0.9 for **1** and **2**. Whether a similar value of this ratio applies to all dipolar and quadrupolar solvents (for **1** and **2**) and to other electron transfer systems remains to be determined. If the correct value of the ratio is substantially different from -1.0, all charge separation reactions in the Marcus normal region will exhibit temperature-dependent rate constants, as the sum $\lambda_S + \Delta G$ can equal zero only at a single temperature. The nonunitary value of the temperature derivative ratio contrasts with the solvent dependence data where changes in λ_S among solvents are attended by nearly identical changes in $-\Delta G$. The reason for the different correlations obtained upon changing solvents and changing temperature is not obvious. Understanding the factors that control each of these ratios would greatly simplify the task of extracting estimates of electronic coupling matrix elements from electron-transfer kinetics.[9]

How well does a continuum model (eq 2) reproduce the experimentally determined λ_S? For any one solvent, perfect agreement with λ_S(300 K) can be obtained by adjusting μ^2/a^3. However, for **1** in dioxane and benzene, unreasonably large μ^2/a^3 (~50 eV) are required to reproduce the experimental λ_S. With $\mu = 15$ D,[15] this yields a cavity radius of 1.4 Å. This failure of the continuum model arises from its description of the solvent response (polarization) in terms of the refractive index and dielectric constant. The latter reflects only the permanent and induced dipole moments of the solvent. As a consequence, solvation arising from short range electrostatic solvent properties, e.g., quadrupole moments, is not accounted for. The continuum model is moderately successful in reproducing λ_S(300 K) in dipolar solvents. For acetonitrile, tetrahydrofuran, and ether, μ^2/a^3 values of 1.7, 2.1, and 1.3 eV, respectively, are needed. Accordingly, either μ or a must vary with solvent,[31] a condition not implemented in simple continuum models, but included in more elaborate variations.[7c,32] The utility of these solvent-dependent μ^2/a^3 values may be checked by using them to predict $\partial\lambda_S/\partial T$. Including only the temperature dependence of the dielectric constant[21] and the refractive index[33] within eq 2, the calculated values of $\partial\lambda_S/\partial T$ are $+0.11$, -0.47, and -0.48 meV/K using the forementioned values of μ^2/a^3 in acetonitrile, tetrahydrofuran, and ether, respectively. The magnitudes of these predicted temperature derivatives differ by more than a factor of 2 from the data in Table 4. Moreover, the continuum prediction and experimental $\partial\lambda_S/\partial T$ in acetonitrile have opposite signs. To match the experimental data, the continuum model requires temperature-dependent and solvent-dependent values of μ and/or a. It appears that the simple continuum model (eq 2) does not provide quantitatively useful predictions of either the solvent or the temperature dependence of λ_S for **1**.

Despite the quantitative failure of the solvent response term in continuum models, these models do predict some of the trends observed in the experimental data. As noted in (c) above, the continuum models predict that, for charge separation reactions, differences between λ_S among solvents are equal to the corresponding differences in $-\Delta G$. The dipole model (eq 2) also does a reasonable job of reproducing the dependence of λ_S on the charge transfer distance.[34] Equating the cavity radius to one-half the major axis of an ellipse circumscribing the solute[34] yields $a \sim 4.5$ Å for **1** and 5.6 Å for **2**. With $\mu = 15.1$ D for **1** and 26.4 D for **2**,[34] the predicted value of $\lambda_S(\mathbf{2})/\lambda_S(\mathbf{1})$ is 1.6, slightly larger than the average experimental value.

How well does a molecular solvation model reproduce the experimental results? Matyushov and Voth[11d] recently published a model for solvation and solvent reorganization energies that represents the solvent as a hard sphere liquid and accounts for solvent molecule polarizability, dipole and quadrupole moments.

TABLE 4: Temperature Dependence of ΔG ($S_0 \rightarrow$ CT) and λ_S for 1 and 2

solvent	$\partial\Delta G/\partial T$(**1**) (eV/$10^3$ K)	$\partial\lambda_S/\partial T$(**1**) (eV/$10^3$ K)	$\partial\Delta G/\partial T$(**2**) (eV/$10^3$ K)	$\partial\lambda_S/\partial T$(**2**) (eV/$10^3$ K)
2-methylbutane	0.18 ± 0.04	0.22 ± 0.04	0.76 ± 0.17	0.26 ± 0.17
diethyl ether	1.36 ± 0.07	-0.99 ± 0.07	1.93 ± 0.09	-1.30 ± 0.09
benzene	1.06 ± 0.07	-0.74 ± 0.07	[a]	[a]
dioxane	1.12 ± 0.05	-0.74 ± 0.05	1.44 ± 0.09	-1.34 ± 0.09
tetrahydrofuran	1.92 ± 0.01	-1.67 ± 0.01	2.04 ± 0.08	-1.44 ± 0.08
acetonitrile	1.06 ± 0.03	-0.72 ± 0.03	0.93 ± 0.09	-0.44 ± 0.09

[a] Not determined.

TABLE 5: λ_S(300 K) and $\partial\lambda_S/\partial T$ Determined from Fits of the Franck−Condon Emission Band

solvent	λ_S(**1**) (300 K) (eV)	$\partial\lambda_S(1)/\partial T$ (eV/10^3 K)	λ_S(**2**) (300K) (eV)	$\partial\lambda_S(2)/\partial T$ (eV/10^3 K)
diethyl ether	0.34 ± 0.02	-0.65 ± 0.30[a]	0.42 ± 0.01	-1.6 ± 0.2
benzene	0.36 ± 0.01	-0.91 ± 0.14	[b]	[b]
dioxane	0.42 ± 0.02	-0.91 ± 0.09	0.55 ± 0.01	-1.4 ± 0.1
tetrahydrofuran	0.50 ± 0.02	-1.8 ± 0.3	0.69 ± 0.02[c]	-1.4 ± 0.3[c]
acetonitrile	0.62 ± 0.01	-0.79 ± 0.05	0.90 ± 0.02	-1.2 ± 0.2

[a] The values of $\lambda_S(T)$ determined by band-shape fitting in this case exhibit considerable scatter. [b] Not determined. [c] The calculated line shapes are of moderate quality in this solvent.

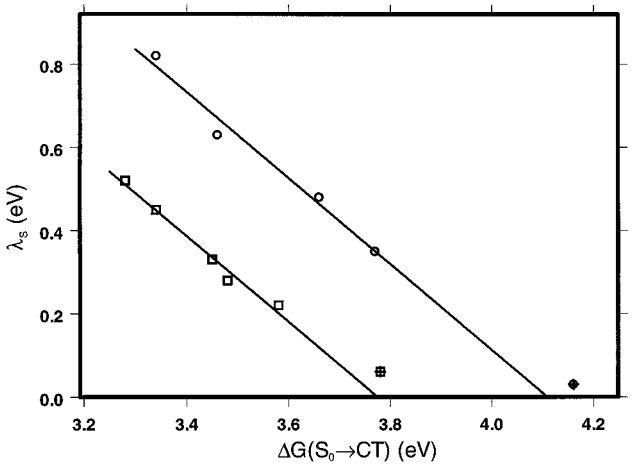

Figure 4. Linear Regression Plots of λ_S vs $\Delta G°$ ($S_0 \rightarrow$ CT) for **1** (□) and **2** (○). The data for 2-methylbutane (square and circle with the inscribed +) are not included in the regression analyses.

Both solvent reorientation and density fluctuations are included in the model. The solute is represented as a hard sphere. The electron transfer event is modeled as a change in an imbedded point dipole moment. As in the continuum model, the solute hard sphere radius is modified to reproduce the experimental λ_S. For **1**, the value of the radius required to duplicate λ_S (Table 5) varies with solvent: from 3.6 Å in ethyl ether to 4.5 Å in acetonitrile (see the Supporting Information for the parameters employed in the fitting). The inclusion of solvent quadrupole moments in the model does a good job of accounting for the observed λ_S in solvents where quadrupole contributions are significant. The required value of the solute radius is 4.0 Å in benzene, 4.3 Å in dioxane, and 4.2 Å in THF. With the solute radius determined by fitting λ_S, the model predicts the solvation energy contribution, $\Delta\Delta G_{SOLV} = \Delta G_{SOLV}(CT) - \Delta G_{SOLV}(S_0)$, to the free energy gap, where $\Delta G(S_0 \rightarrow CT)_{experiment} = \Delta G(S_0 \rightarrow CT)_{VACUUM} + \Delta\Delta G_{SOLV}$. The predicted value of $\Delta G(S_0 \rightarrow CT)_{VACUUM}$ from each solvent falls between 4.3 and 4.4 eV. This value is reasonable given available IP and EA data.[35] A plot (analogous to Figure 4) of λ_S versus $\Delta\Delta G_{SOLV}$ (predicted) for the five solvents is linear with a slope of −0.8, not −1.0 (vide supra). Considering the range of solvents used, Matyushov's model[11d] does a good job of reproducing the room-temperature data from **1**.

This molecular solvation model was also used to determine the solute radius needed to reproduce λ_S for **2** (Table 5). The radii are 4.9 Å in ether, 5.5 Å in dioxane and THF, and 5.8 Å in acetonitrile. As for **1**, the radius required to duplicate λ_S for **2** in ether is considerably smaller than for the other solvents. Fixing the cavity radius at 5.6 Å produces λ_S estimates within 0.1 eV of the experimental values: 0.29 eV (ether), 0.51 eV (dioxane), 0.65 eV (THF), 1.0 eV (acetonitrile). The corresponding values of $\Delta\Delta G_{SOLV}$ (vida supra) require $\Delta G(S_0 \rightarrow CT)_{VACUUM} = 4.4-4.5$ eV. For both solutes, the molecular solvation model[11d] does a reasonable job of estimating room-temperature reorganization and solvation energies across a wide range of solvents.

Using the *best fit radii* for **1**, the molecular solvation model's predictions of $\partial\lambda_S/\partial T$ and $\partial\Delta G/\partial T$ are too steep in every solvent except acetonitrile. The ratio of the predicted to the experimental slopes vary monotonically with increasing polarity: 2.5−3.0 in ether, 1.1−1.7 in THF, and 0.8−1.2 in acetonitrile (see Supporting Information). Although the predicted slopes are too large, the predicted values of $(\partial\lambda_S/\partial T)/(\partial\Delta G/\partial T)$ are close to −0.6, in reasonable agreement with the experimental finding. There is a rough correlation between the solute hard sphere radius and the "excess" of the predicted slopes. Use of 4.5 Å as the solute radius yields temperature derivatives that are in better agreement with experimental data, but produces estimates of λ_S that are 0.1 eV too small in THF, dioxane, and benzene and 0.17 eV too small in ether. The molecular solvation model overestimates the magnitudes of $\partial\lambda_S/\partial T$ and $\partial\Delta G/\partial T$ in **2**, by as much as 2-fold, when the solute radius is chosen to reproduce the experimental λ_S(300 K) value in each solvent. As for **1**, the predicted temperature derivatives for **2** are closest to the experimental values in acetonitrile. Fixing the solute radius at 5.6 Å produces temperature derivative estimates that are, generally, within 25% of the experimental results (Results in Supporting Information). The aforementioned analyses were performed using a state-independent value of the solute polarizability. Increasing the polarizability of **1**'s CT state, relative to the S_0 state, results in larger values of the solute radius (when fitting λ_S) and reduces the predicted magnitudes of the temperature derivatives. A larger value of the CT state polarizability is predicted[36] to generate an emission line shape that is wider than the absorption line shape, in accordance with the experimental observations (Figure 2). In the future, we will explore

whether the introduction of a state-dependent polarizability enables Matyushov's model[11d] to reproduce the temperature and solvent dependence of the absorption and emission spectral data using a single solute radius.

The quantitative aspects of the above conclusions and discussion rely on three approximations made in processing the excitation and emission spectra: (1) the Stokes shift is equal to $2\lambda_S + 2\lambda_V$; (2) the transition dipole moment for both transitions is given by $(\Delta\mu\ V(S_0 \rightarrow CT)/(h\nu))$, where $\Delta\mu$ is the difference of the S_0 and CT state dipole moments, V is the electronic coupling matrix element, and ν is the transition frequency; (3) λ_V and λ_S are identical on the S_0 and CT potential surfaces. Each of these approximations can be challenged. (1) The Stokes shift is equal to $2\lambda_S + 2\lambda_V$ only if λ_V includes negligible contributions from high frequency (>200 cm^{-1}) quantized modes. Mertz[24] calculated various moments of CT spectra and concluded that one-half the Stokes shift is equal to $\lambda_S + \lambda_V - \hbar\omega/2(1 + (k_BT\lambda_S/\hbar\omega\lambda_V))$ for a single quantized mode model. For $\lambda_V = 0.45$ eV and $\hbar\omega = 0.225$ eV, the λ_S value extracted from the Stokes shift data is predicted to be 0.1 eV too small between 250 and 350 K. This prediction is in reasonable agreement with the 0.08 eV difference of the λ_S(**1**) entries in Tables 3 and 5. Provided the single quantized mode model for the CT spectrum is appropriate, the entries in Table 5 are more appropriate than those in Tables 3 and 4. The differences are quantitatively and qualitatively small and do not obviate the conclusions drawn above.

(2) Verhoeven and co-workers provided evidence of oscillator strength borrowing from the dicyanoethylene $S_0 \rightarrow S_1$ transition in the CT absorption[17] band of **1** and in the emission[37] spectrum of a related compound. If all the CT intensity is borrowed, the appropriate 3-state model transition moment[37,38] is $(\mu^*\ V^*(S_1 \rightarrow CT)/(E_1 - h\nu))$ where μ^* is the $S_0 \rightarrow S_1$ transition dipole moment, E_1 is the dicyanoethylene zero−zero transition energy, and V^* is the $S_1 \rightarrow$ CT electronic coupling matrix element. The excitation and emission spectra from **1** were reduced using this transition moment expression ($E_1 = 43.9$ kK[37]) and λ_S and ΔG were evaluated using eqs 3 as described in the Experimental Section. The λ_S values obtained with the three-state model were slightly larger (0.06 ± 0.02 eV) than the values reported in Table 3. The $\Delta G(S_0 \rightarrow CT)$ values obtained using the three-state model were smaller than the corresponding entries in Table 3. In contrast to the λ_S results, the difference between ΔG from the three-state and two-state models varied monotonically with solvent polarity; from −0.18 eV in acetonitrile to −0.14 eV in benzene. The temperature derivatives of λ_S and ΔG obtained with the three-state model were similar to the results in Table 4, with $(\partial\lambda_S/\partial T)/(\partial\Delta G/\partial T) = -0.76 \pm 0.05$ for **1**. With respect to all quantities evaluated in this investigation, use of the three-state transition moment models slightly alters the quantitative results but none of the qualitative conclusions drawn above are challenged.

(3) If λ_S and λ_V are the same for both the CT and ground-state surfaces, the reduced CT excitation and emission spectra should be mirror images. Figure 2 clearly demonstrates that the excitation band is narrower than the emission band. λ_V may be different on the two surfaces. Alternatively, Matyushov and Voth[36] showed that λ_S varies depending on the polarizability of the state (ground or CT). For small donor and acceptor groups, such as in **1** and **2**, electron transfer could significantly alter the polarizability. If a change in polarizability is the source of the different widths, the procedure employed here defines an average λ_S.

V. Summary

The dependence of the free energy gap, $\Delta G(S_0 \rightarrow CT)$, and of the solvent reorganization energy, λ_S, on solvent, donor/acceptor separation, and temperature were determined from analyses of the intramolecular charge transfer absorption and emission bands present in **1** and **2**. For either probe molecule, differences in the CT state energy among solvents are attended by nearly identical magnitude (but opposite sign) differences in the solvent reorganization energy. This correlation is observed for solvents in which the most significant electrostatic contributor is the dipole or the quadrupole moment. Solvents with nearly zero dipole moments but large quadrupole moments ($\langle Q \rangle$ = 8−11 D-Å) solvate the CT state as effectively as moderately dipolar solvents ($\mu \approx 1-2$ D). Larger charge separation distances produce larger solvent reorganization energies in the nonalkane solvents. The ratio of the solvent reorganization energies for **2** and **1**, λ_S(**2**)/λ_S(**1**), is roughly the same in the dipolar and quadrupolar solvents. Changes in both ΔG and λ_S upon increasing the temperature are consistent with a decrease in the solvent polarity. In contrast to the nearly identical variation of λ_S and $-\Delta G$ with solvent, the change of λ_S with temperature is 70−90% of that found for $-\Delta G$ (in any one solvent).

Simple continuum models, employing solvent- and temperature-independent cavity radii, are not of quantitative use in explaining or predicting the solvent and temperature dependence of λ_S and ΔG. The continuum model's expression of solvation energy (polarity) in terms of dielectric constants fails to be of even qualitative use in solvents possessing large quadrupole and small dipole moments. Despite the quantitative failures of these models, some of the more broadly viewed continuum predictions for charge separation reactions are upheld by this study, e.g., nearly identical magnitude changes in λ_S and $-\Delta G$ with solvent variation and solvent-independent variation (on a percentage basis) of the solvent reorganization energy as a function of charge transfer distance (eq 2).

A molecular solvation model that attributes solvent molecules' dipole moment, quadrupole moment, and polarizability to a liquid of hard spheres was also applied to the data. The incorporation of quadrupole moments into the model drastically improves the accuracy of the solvation and reorganization energies predicted across a wide variety of solvents using a single value of the solute radius. Nonetheless, quantitative agreement with the experimental data required moderate differences in the best-fit value of the solute radius for each solvent. The model significantly overestimates the temperature derivatives λ_S and $\Delta G(S_0 \rightarrow CT)$ in weakly polar solvents, but the agreement with experiment improves as the solvent polarity increases. The model's predictions of the ratios between various reorganization and solvation energy quantities are in reasonable agreement with the experimental results. Overall, the molecular solvation model produces considerably better estimates of reorganization and solvation energies, as a function of solvent and temperature, than are produced by continuum models.

Acknowledgment. We thank the National Science Foundation for financial support. We gratefully acknowledge informative discussions with Professor David H. Waldeck (University of Pittsburgh) and Dr. Dmitry Matyushov (University of Utah). We also gratefully acknowledge the use of software developed by Dr. Matyushov.

Supporting Information Available: Two charge transfer emission spectra: **1** in MeCN at 333 K and **2** in ether at 245 K; one table with parameters and results from the use of

Matyushov's Model for solvation and solvent reorganization energies. This material is available free of charge via the Internet at http://pubs.acs.org.

References and Notes

(1) Marcus, R. A.; Sutin, N. *Biochim. Biophys. Acta* **1985**, *811*, 265.

(2) (a) Marchi, M.; Gehlen, J. N.; Chandler, D.; Newton, M. *J. Am. Chem. Soc.* **1993**, *115*, 4178. (b) Warshel, A.; Hwang, J.-K. *J. Chem. Phys.* **1986**, *84*, 4938. (c) Zhou, H.-X.; Szabo, A. *J. Chem. Phys.* **1995**, *103*, 3481.

(3) (a) Marcus, R. A. *Annu. Rev. Phys. Chem.* **1964**, *15*, 155. (b) Matyushov, D. V.; Schmid, R. *J. Chem. Phys.* **1996**, *105*, 4729. (c) Matyushov, D. V. *Mol. Phys.* **1993**, *79*, 795.

(4) (a) Blackbourn, R. L.; Hupp, J. T. *J. Phys. Chem.* **1988**, *92*, 2817. (b) Hupp, J. T.; Dong, Y.; Blackbourn, R. L.; Lu, H. *J. Phys. Chem.* **1993**, *97*, 3278. (c) Dong, Y.; Hupp, J. T. *Inorg. Chem.* **1992**, *31*, 3322. (d) Hush, N. S. *Prog. Inorg. Chem.* **1967**, *8*, 391. (d) Derr, D. L.; Elliott, C. M. *J. Phys. Chem. A* **1999**, *103*, 7888.

(5) (a) Nelsen, S. F.; Trieber, D. A., II; Wolff, J. J.; Powell, D. R.; Rogers-Crowley, S. *J. Am. Chem. Soc.* **1997**, *119*, 6873. (b) Nelsen, S. F.; Ismagilov, R. F.; Trieber, D. A., II. *Science* **1997**, *278*, 846.

(6) (a) Gould, I. R.; Young, R. H.; Moody, R. E.; Farid, S. *J. Phys. Chem.* **1991**, *95*, 2068. (b) Walker, G. C.; Åkesson, E.; Johnson, A. E.; Levinger, N. E.; Barbara, P. F. *J. Phys. Chem.* **1992**, *96*, 3728. (c) Meyers-Kelley, A. *J. Phys. Chem. A.* **1999**, *103*, 6891.

(7) (a) Marcus, R. A.; *J. Chem. Phys.* **1956**, *24*, 966. (b) Allen, G. C.; Hush, N. S. *Prog. Inorg. Chem.* **1967**, *8*, 357. (c) Newton, M. D.; Basilevsky, M. V.; Rostov, I. V. *Chem. Phys.* **1998**, *232*, 201. (d) Matyushov, D. V. *Chem. Phys.* **1996**, *211*, 46. (e) Jonggu, J.; Kim, H. J. *J. Chem. Phys.* **1997**, *106*, 5979.

(8) Vath, P.; Zimmt, M. B.; Matyushov, D. V.; Voth, G. A. *J. Phys. Chem. B* **1999**, *103*, 9130.

(9) Kumar, K.; Kurnikov, I. V.; Beratan, D. N.; Waldeck, D. H.; Zimmt, M. B. *J. Phys. Chem. A* **1998**, *102*, 5529.

(10) (a) Papazyan, A.; Warshel, A. *J. Chem. Phys. B* **1997**, *101*, 11254. (b) Matyushov, D.; Ladanyi, B. M. *J. Chem. Phys.* **1999**, *110*, 994.

(11) (a) Reynolds, L.; Gardecki, J. A.; Frankland, S. J. V.; Horng, M. L.; Maroncelli, M. *J. Phys. Chem.* **1996**, *100*, 10337. (b) Perng, B.-C.; Newton, M. D.; Raineri, F. O.; Friedman, H. L. *J. Chem. Phys.* **1996**, *104*, 7177−7204. (c) Perng, B.-C.; Newton, M. D.; Raineri, F. O.; Friedman, H. L. *J. Chem. Phys.* **1996**, *104*, 7153−7176. (d) Matyushov, D. V.; Voth, G. A. *J. Chem. Phys.* **1999**, *111*, 3630.

(12) (a) Wegewijs, B.; Paddon-Row, M. N.; Braslavsky, S. E. *J. Phys. Chem. A* **1998**, *102*, 8812. (b) Morais, J.; Zimmt, M. B. *J. Phys. Chem.* **1995**, *99*, 8863.

(13) Matyushov, D. *Chem. Phys.* **1993**, *174*, 199.

(14) (a) Matyushov, D. V.; Schmid, R.; Ladanyi, B. M. *J. Phys. Chem.* **1997**, *101*, 1035. (b) Matyshov, D. V.; Schmid, R. *J. Chem. Phys.* **1995**, *103*, 2034.

(15) Equation 1: This Marcus expression for λ_S applies to the transfer of a single electron across a distance R_{CC} from a donor of radius r_D to an acceptor of radius r_A in a solvent of refractive index n and static dielectric constant ϵ_S. In the dipole expression for λ_S (eq 2), μ is the change in dipole moment from the initial to the final state, a is the cavity radius, and the solvent parameters are as described for eq 1.

(16) (a) Yelle, R. B.; Ichiye, T. *J. Phys. Chem. B* **1997**, *101*, 4127. (b) Hwang, J. K.; Warshel, A. *J. Am. Chem. Soc.* **1987**, *109*, 715.

(17) Pasman, P.; Rob, F.; Verhoeven, J. W. *J. Am. Chem. Soc.* **1982**, *104*, 5127.

(18) Louis-Andre, O.; Gelbard, G. *Tetrahedron Lett.* **1985**, *26*, 831−832.

(19) Marcus, R. A. *J. Phys. Chem.* **1989**, *93*, 3078.

(20) Fitting the CT emission spectrum by itself leads to considerable correlation between ΔG and λ_S. See also (a) Gould, I. R.; Farid, S. *J. Phys. Chem.* **1992**, *96*, 7635. (b) Zeng, Y.; Zimmt, M. B. *J. Phys. Chem.* **1992**, *96*, 8395.

(21) Marcus, Y. *Ion Solvation*; Wiley and Sons: Chichester, 1985; pp 133−144.

(22) Closs, G. L.; Calcaterra, L. T.; Green, N. J.; Penfield, K. W.; Miller, J. R. *J. Phys. Chem.* **1986**, *90*, 3673.

(23) Under the assumption that λ_S is zero in 2-methylbutane, the proper λ_S values are 0.07 eV smaller for **1** and 0.03 eV smaller for **2**.

(24) (a) Mertz, E. L.; Vyacheslav, A. T.; Krishtalik, L. I. *J. Phys. Chem. A* **1997**, *101*, 3433. (b) Mertz, E. L. *Chem. Phys. Lett.* **1996**, *262*, 27.

(25) The ability of quadrupolar solvents to stabilize dipolar species depends both on the solvent quadrupole moment and the solvent size, as $\langle Q\rangle^2/\sigma^5$, where $\langle Q\rangle$ is the effective axial quadrupole moment and σ is the solvent's hard sphere diameter.[11d] The literature[31b] diameter of ether, benzene, dioxane, and THF are very similar (see Supporting Information). The diameters of acetonitrile and methylbutane are slightly smaller. However, these two solvents have very small quadrupole moments.

(26) The correlation coefficient for a plot of the CT state energy vs $(\epsilon - 1)/(2\epsilon + 1)$ in ether, THF, and acetonitrile is 0.87 for **1** and 0.92 for **2**.

(27) Inclusion of the 2-methylbutane data points yields regression slopes of −0.91 and −0.93 for **1** and **2**, respectively.

(28) (a) Kroon, J.; Verhoeven, J. W.; Paddon-Row, M. N.; Oliver, A. M. *Angew. Chem., Int. Ed. Engl.* **1991**, *30*, 1358. (b) Wasielewski, M. R.; Gaines, G. L.; O'Neil, M. P.; Svec, W. A.; Niemczyk, M. P.; Prodi, L.; Gosztola, D. In *Dynamics and Mechanisms of Photoinduced Electron Transfer and Related Phenomena*; Mataga, N., Okada, T., Masuhara, H., Eds.; Elsevier: Amsterdam, 1992; pp 87−103. (c) This correlation is observed only if the dipole moment of the initial state is much smaller than the dipole moment of the CT state.

(29) Molecular models of solvation predict reduced sensitivity of λ_S to the solvent polarizability (refractive index) as compared to continuum models. See ref 8.

(30) The data indicate that the entropy contribution to ΔG, $-T\Delta S$, is *less* positive for **2** than for **1** in acetonitrile at 300 K. This result is surprising. Although there is no thermodynamic significance to the ratio of two entropies, it is interesting to note that $\Delta S(\mathbf{2})/\Delta S(\mathbf{1})$ decreases with increasing solvent polarity: the ratios (± 0.1) are 1.4 in diethyl ether, 1.3 in dioxane, 1.1 in THF, and 0.9 in acetonitrile.

(31) (a) Using the $S-C_4$ separation in **1** as the (solvent-independent) CT distance, $\Delta\mu = 15.1$ D. The continuum model cavity radius needed to reproduce the experimental λ_S value for **1** is 4.37, 4.06, and 4.73 Å in MeCN, THF, and ether, respectively. This solvent dependence is not explained simply by including the diameter of the solvent molecule in the expression for the cavity radius: $R_{eff} = R_{HS} + \sigma/2$, where R_{HS} is the hard sphere radius of the probe and σ is the hard sphere diameter of the solvent (see refs 3b,c, 7c−e, 32). The solvent dependence of the σ values for these three solvents, 4.27, 5.08, and 5.25 Å, respectively, does not match the above-noted solvent dependence of the cavity radius.[31b] (b) Schmid, R.; Matyushov, D. V. *J. Phys. Chem.* **1995**, *99*, 2393.

(32) Fawcett, W. R.; Blum, L. *Chem. Phys. Lett.* **1991**, *187*, 173.

(33) Wohlfarth, Ch.; Wohlfarth, B. *Refractive indices of pure liquids and binary liquid mixtures*, Electronic Version of Landolt Börnstein, Vol. III/38; Martienssen, W., Ed.; Springer: Berlin, 1996.

(34) It is straightforward to test eq 2. The dipole moment (units of Debye) is equated to 4.8 times the $S-C_4$ separation (Å), where C_4 is the ring-substituted alkene C: 3.15 Å in **1** and 5.49 Å in **2**. The dipole moment calculated in this manner for **1**, 15.1 D, is very close to the $S_0 \rightarrow$ CT change in the dipole moment calculated theoretically. The equation of the circumscribing ellipse was determined from the coordinates of the most remote points on the van der Waals surface of the S and the two N atoms. The coordinates were obtained using Personal CAChe, Oxford Molecular, Version 2.1, 1996. The radii were equated to one-half the major axis. A similar test of eq 1 is not possible. There is not an unambiguous means to define the donor and acceptor radii and the coordinates of the charge centers. Slight changes in these quantities lead to widely different values of $\lambda_S(\mathbf{2})/\lambda_S(\mathbf{1})$.

(35) (a) $\Delta G(S_0 \rightarrow CT)_{VACUUM}$ may be estimated from the donor ionization potential, the acceptor electron affinity, and the Coulomb interaction between the oxidized donor and reduced acceptor. The gas-phase ionization potential of 4-methylene thiacyclohexane derivatives range between 9.2 and 9.3 eV.[35b] Use of the S to C-4 separation of 3.15 Å to estimate the Coulomb interaction yields −4.6 eV. Thus, the electron affinity of the acceptor group would need to be 0.2 to 0.3 eV to obtain the derived $\Delta G(S_0 \rightarrow CT)_{VACUUM}$ value of 4.3−4.4 eV. Unfortunately, EA data for 1,1-dicyanoethylene derivatives were not found. Burrow and co-workers[35c] posited a vertical electron affinity in acrylonitrile of −0.1 eV and in fumaronitrile of 1.8 eV. Cross conjugation involving the two nitrile groups in **1** and the presence of the alkyl ring should produce an EA that is between 0 and 1 eV. (b) Sarneel, R.; Worrell, C. W.; Pasman, P.; Verhoeven, J. W.; Mes, G. F. *Tetrahedron* **1980**, *36*, 3241. (c) Burrow, P. D.; Howard, A. E.; Johnston, A. R.; Jordan, K. J. *J. Phys. Chem.* **1992**, *96*, 7570.

(36) Matyushov D. V.; Voth, G. A. A Theory of Electron Transfer and Steady-State Optical Spectra of Chromophores with Varying Electronic Polarizability. *J. Chem. Phys.*, in press.

(37) Bixon, M.; Jortner, J.; Verhoeven, J. W. *J. Am. Chem. Soc.* **1994**, *116*, 7349.

(38) (a) Gould, I. R.; Young, R. H.; Mueller, L. J.; Albrecht, A. C.; Farid, S. *J. Am. Chem. Soc.* **1994**, *116*, 3147. (b) *ibid*, **1994**, *116*, 8188.